Inorganic Chemistry

Article

pubs.acs.org/IC

Linkage Isomerism in Transition-Metal Complexes of Mixed (Arylcarboxamido)(arylimino)pyridine Ligands

David W. Boyce, Debra J. Salmon, and William B. Tolman*

Department of Chemistry and Center for Metals in Biocatalysis, University of Minnesota, 207 Pleasant Street SE, Minneapolis, Minnesota 55455, United States

Supporting Information

ABSTRACT: The synthesis of a series of asymmetric mixed 2,6-disubstituted (arylcarboxamido)(arylimino)pyridine ligands and their coordination chemistry toward a series of divalent first-row transition metals (Cu, Co, and Zn) have been explored. Complexes featuring both anionic *N*,*N*′,*N*″-carboxamido and neutral *O*,*N*,*N*′-carboxamide coordination have been prepared and characterized by X-ray crystallography, cyclic voltammetry, and UV−visible and EPR spectroscopy. Specifically, ^{R}LM(X) (M = Cu; X = Cl^-, OAc^-) and ^{R}L(H)MX_2 (M = Cu, Co, Zn; X = Cl^-, SbF_6^-) complexes that feature *N*,*N*′,*N*″- or *O*,*N*,*N*′-coordination are presented. Base-induced linkage isomerization from *O*,*N*,*N*′-carboxamide to *N*,*N*′,*N*″-carboxamido coordination is also confirmed by multiple forms of spectroscopy.

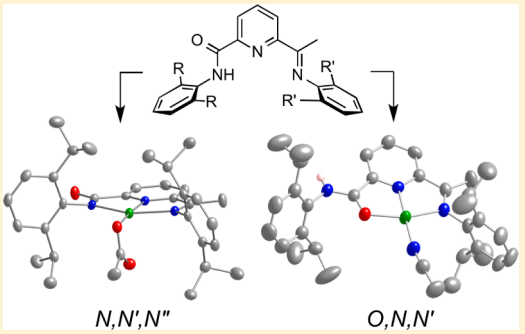

INTRODUCTION

In their doubly deprotonated form, bis(arylcarboxamido)-pyridines **1** have been used as ligands to support nickel and copper complexes that exhibit novel properties. A unique anionic copper(II)−superoxide complex supported by $\mathbf{1}^{2-}$ (R = *i*Pr) acts as a nucleophile, in contrast to other such species supported by neutral N-donor ligands.[1,2] Monoanionic nickel-(II)− and copper(II)−hydroxide complexes supported by $\mathbf{1}^{2-}$ (R = *i*Pr or Me) undergo CO_2 fixation reactions at exceptionally high rates[3] and react with CH_3CN in an unprecedented manner to yield cyanomethide complexes, $[(\mathbf{1}^{2-})M(CH_2CN)]^-$ (R = Me, M = Ni or Cu).[4] In addition, one-electron oxidation of the copper(II)−hydroxide complexes yields thermally unstable Cu(III) species that rapidly oxidize dihydroanthracene via hydrogen atom abstraction (HAT).[4,5] Among the various factors that underlie these unique observations, the dianionic nature and strong electron-donating properties of the supporting ligand $\mathbf{1}^{2-}$ would appear to be key. As part of ongoing studies of these various influences, we asked: What would be the consequences of decreasing the negative charge of the supporting ligand while keeping the steric properties approximately constant?

As a first step toward addressing this question experimentally, we targeted ligands **2a**−**2c** for synthesis and study of their coordination chemistry. These ligands may be viewed as a hybrid of the aforementioned **1** and bis(arylimino)pyridines like **3**, which have been widely studied,[6] including with Cu(II).[7] Ligand **2b** has been reported, but only as a product of an oxidation of a reduced Ni(II) complex of **3**.[8] A direct large-scale synthesis was not described, and **2a** and **2c** are new. Alkyl-substituted analogues **4**, which, in deprotonated form, would be expected to be more basic than monoanionic versions **2a**−**2c**, have been used to prepare Ni(II), Pd(II), and Fe(II) catalysts (e.g., for olefin polymerizations).[9] Ligands **5**[10] and **6**[11] are noteworthy relatives of **2a**−**2c**, insofar as they contain similar tridentate, *mer*, monoanionic N-donor sets.

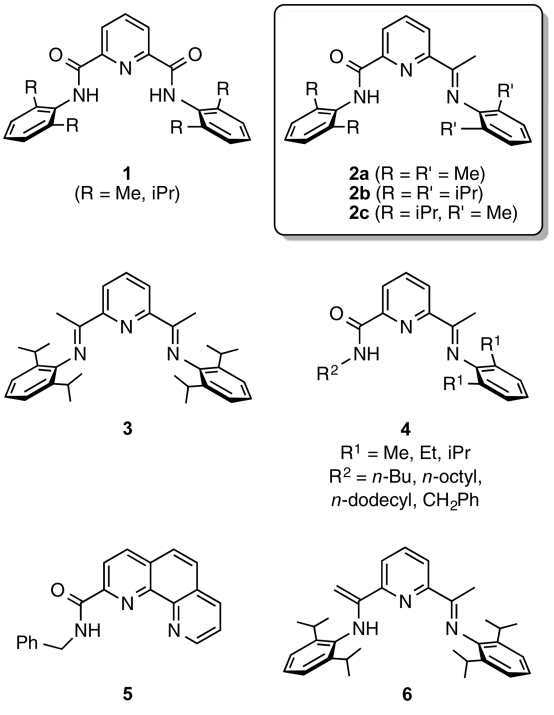

Received: March 19, 2014
Published: May 12, 2014

   dx.doi.org/10.1021/ic500638z | *Inorg. Chem.* 2014, 53, 5788−5796

Herein, we report reproducible, large-scale synthetic routes to **2a**–**2c** and the results of explorations of their ability to complex to divalent metal ions, with an emphasis on Cu(II). We found that metalations in the absence of base result in complexes that exhibit carboxamide *O,N,N′*-coordination and that subsequent treatment of these compounds with base induces isomerization to carboxamido *N,N′,N″*-coordination. The structural and spectroscopic characterization of the complexes provides a foundation for future studies of biomimetic and/or catalytic reactivity.

RESULTS AND DISCUSSION

Synthesis and Characterization of Ligands and *N,N′,N″*-Bound Complexes ^{R}LCuX (X = Cl^{-}, OAc^{-}). The report of ^{iPr2}L(H) (**2b**)[8] sparked our interest in arylcarboxamido(arylimino)pyridine ligands and motivated the development of a large-scale synthesis that could be modified to enable access to a series of related ligands with variable aryl substitution. We found that treatment of 6-acetylpicolinic acid with oxalyl chloride, followed by the desired aniline in the presence of NEt_3, yielded ketocarboxamide precursors **7** (Scheme 1). Addition of **7a** or **7b** to a preformed mixture of

Scheme 1

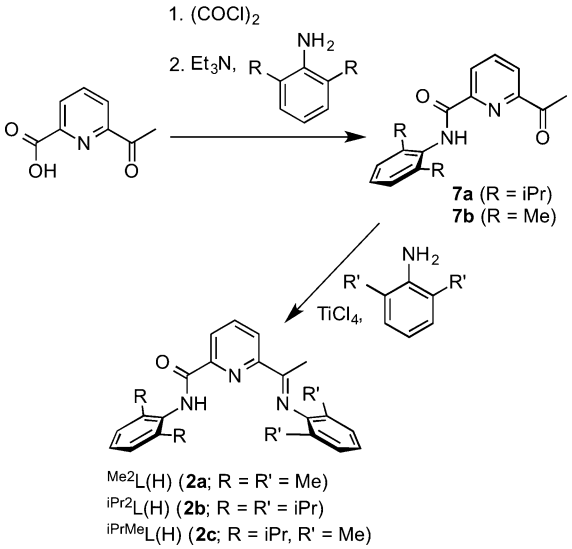

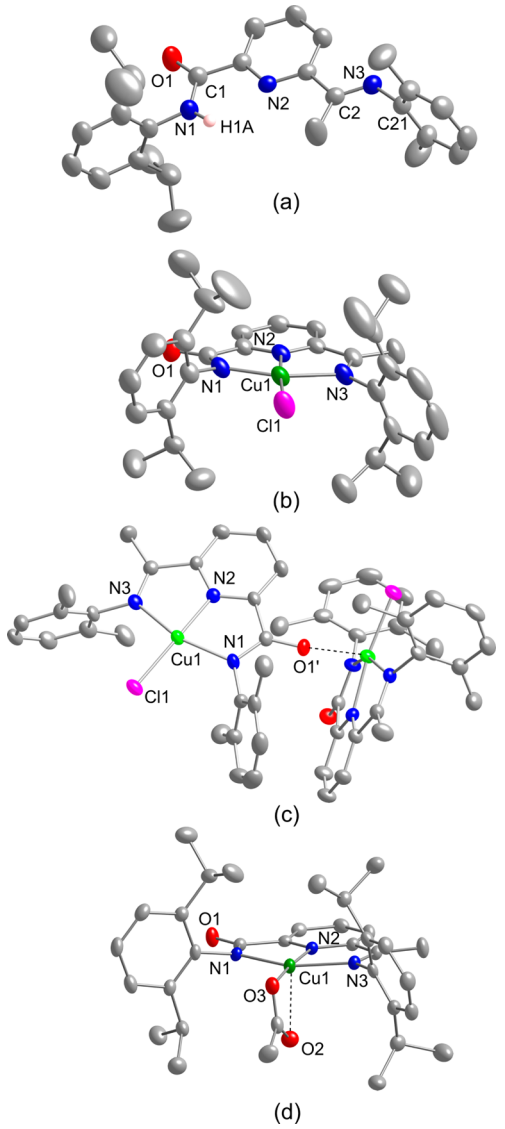

Figure 1. Representations of the X-ray crystal structures of (a) ^{iPrMe}L(H) (**2c**), (b) ^{iPr2}LCuCl (**8b**), (c) ^{Me2}LCuCl (**8a**), and (d) ^{iPr2}LCuOAc (**9b**), showing all non-hydrogen atoms as 50% thermal ellipsoids. See Table 1 for selected interatomic distances and angles.

$TiCl_4$ and the second aniline provided ^{R}L(H) (**2a**–**2c**) in a total yield of up to 47%. The indicated formulations for **7a**,**7b** and **2a**–**2c** were supported by ^{1}H and ^{13}C NMR spectroscopy and, in the case of ^{iPrMe}L(H) (**2c**), X-ray crystallography. In the X-ray crystal structure of **2c**, the amide, pyridine, and imine moieties are coplanar, but with the imine donor facing away from the putative metal ion binding pocket (Figure 1a and Table 1).

Treatment of ^{R}L(H) (**2a**–**2c**) with sodium methoxide in the presence of $CuCl_2$ yielded complexes ^{R}LCuCl (**8a**–**8c**) (Scheme 2). Related complexes ^{R}LCuOAc (**9b**,**9c**) were synthesized by refluxing ^{iPr2}L(H) (**2b**) or ^{iPrMe}L(H) (**2c**), respectively, with $Cu(OAc)_2{\cdot}H_2O$ in MeCN. The formulations of all of these compounds are supported by UV–vis and EPR spectroscopy, ESI mass spectrometry, and X-ray crystallographic data (**8a**, **8b**, and **9b** in Figure 1; **8c** and **9c** in Figure S2, Supporting Information). Similar *N,N′,N″*-coordination of their arylcarboxamido(arylimino)pyridine ligands is apparent in all of the X-ray structures, each of which shows a tetragonal geometry for the Cu(II) ion. Disparate Cu–N bond distances within each complex are seen, with the trend Cu–N(pyridyl) < Cu–N(amide) < Cu–N(imine) reflected by the average distances of 1.927, 1.980, and 2.100 Å, respectively. The observation of the shortest Cu–N bond for the pyridyl group is consistent with previously reported structures of complexes of bis(arylcarboxamido)pyridine or diiminopyridine ligands **1** and **3**.[12] Apparently, as a result of decreased steric bulk of its methyl-substituted aryl groups, the X-ray structure of ^{Me2}LCuCl (**8a**) is composed of polymeric repeating units resulting from axial coordination of the carboxamide carbonyl of one "monomer" to the copper center of a neighboring unit (**8a**; Cu1–O1′1 = 2.345(3) Å) (Figure 1c). Similar axial coordination, albeit intramolecular and involving an acetate ligand O atom, is observed in *i*Pr$_2$LCuOAc (**9b**; Cu1–O2 = 2.369(2) Å; Figure 1d) and ^{iPrMe}LCuOAc (**9c**; Cu1–O3 = 2.456(3) Å; Figure S6b, Supporting Information).

dx.doi.org/10.1021/ic500638z | Inorg. Chem. 2014, 53, 5788–5796

Table 1. Selected Interatomic Distances (Å) and Angles (deg) for the Indicated X-ray Crystal Structures[a]

^{iPrMe}L(H) (**2c**)				^{Me2}LCuCl (**8a**)			
N(1)−C(1)	1.344(3)	O(1)−C(1)−N(1)	124.0(3)	Cu(1)−N(1)	2.005(3)	N(2)−Cu(1)−N(1)	80.18(12)
O(1)−C(1)	1.223(3)	N(1)−C(1)−C(3)	114.2(2)	Cu(1)−N(2)	1.934(3)	N(2)−Cu(1)−N(3)	77.58(11)
C(2)−N(3)	1.260(3)	N(3)−C(2)−C(8)	126.6(2)	Cu(1)−N(3)	2.130(3)	N(1)−Cu(1)−N(3)	154.56(11)
		C(2)−N(3)−C(21)	122.6(2)	Cu(1)−Cl(1)	2.2092(10)	N(2)−Cu(1)−Cl(1)	172.53(9)
				Cu(1)−O(1)′	2.345(3)	N(1)−Cu(1)−Cl(1)	102.41(9)
						N(3)−Cu(1)−Cl(1)	98.25(8)
^{iPr2}LCuCl (**8b**)				^{iPrMe}LCuCl (**8c**)			
Cu(1)−N(1)	1.960(3)	N(2)−Cu(1)−N(1)	81.68(10)	Cu(1)−N(1)	1.962(3)	N(2)−Cu(1)−N(1)	81.14(12)
Cu(1)−N(2)	1.939(2)	N(2)−Cu(1)−N(3)	77.43(10)	Cu(1)−N(2)	1.926(3)	N(2)−Cu(1)−N(3)	77.92(12)
Cu(1)−N(3)	2.098(3)	N(1)−Cu(1)−N(3)	159.01(10)	Cu(1)−N(3)	2.070(3)	N(1)−Cu(1)−N(3)	158.74(12)
Cu(1)−Cl(1)	2.1923(9)	N(2)−Cu(1)−Cl(1)	175.40(8)	Cu(1)−Cl(1)	2.1755(10)	N(2)−Cu(1)−Cl(1)	173.84(9)
		N(1)−Cu(1)−Cl(1)	102.31(8)			N(1)−Cu(1)−Cl(1)	102.66(9)
		N(3)−Cu(1)−Cl(1)	98.65(8)			N(3)−Cu(1)−Cl(1)	98.52(9)
^{iPr2}LCuOAc (**9b**)				^{iPrMe}LCuOAc (**9c**)			
Cu(1)−N(1)	1.999(3)	N(2)−Cu(1)−O(3)	174.69(10)	Cu(1)−N(1)	1.974(2)	N(2)−Cu(1)−O(2)	167.88(11)
Cu(1)−N(2)	1.913(3)	N(2)−Cu(1)−N(1)	81.39(11)	Cu(1)−N(2)	1.923(2)	N(2)−Cu(1)−N(1)	81.31(9)
Cu(1)−N(3)	2.127(3)	O(3)−Cu(1)−N(1)	103.75(10)	Cu(1)−N(3)	2.075(2)	O(2)−Cu(1)−N(1)	103.56(10)
Cu(1)−O(2)	2.369(2)	N(2)−Cu(1)−N(3)	78.02(10)	Cu(1)−O(2)	1.932(2)	N(2)−Cu(1)−N(3)	78.15(9)
Cu(1)−O(3)	1.921(2)	O(3)−Cu(1)−N(3)	97.06(10)	Cu(1)−O(3)	2.456(3)	O(2)−Cu(1)−N(3)	96.17(10)
		N(1)−Cu(1)−N(3)	157.92(10)			N(1)−Cu(1)−N(3)	159.32(9)
		N(2)−Cu(1)−O(2)	117.31(10			N(2)−Cu(1)−O(3)	134.20(11)
		O(3)−Cu(1)−O(2)	60.32(9)			O(2)−Cu(1)−O(3)	55.70(11)
[^{iPr2}L(H)Cu(MeCN)][$(SbF_6)_2$] (**10**)				[^{iPrMe}L(H)Cu(H_2O)THF][$(SbF_6)_2$] (**12**)			
Cu(1)−O(1)	1.9910(16)	N(2)−Cu(1)−O(1)	81.21(7)	Cu(1)−O(1)	2.044(2)	N(2)−Cu(1)−O(1)	79.79(9)
Cu(1)−N(3)	2.0223(19)	N(4)−Cu(1)−N(3)	97.95(8)	Cu(1)−N(2)	1.912(2)	N(2)−Cu(1)−O(2)	165.24(10)
Cu(1)−N(4)	1.921(2)	O(1)−Cu(1)−N(3)	161.66(7)	Cu(1)−O(2)	1.914(2)	O(2)−Cu(1)−O(1)	95.64(9)
Cu(1)−N(2)	1.8938(19)	N(2)−Cu(1)−N(4)	177.88(9)	Cu(1)−N(3)	2.067(2)	N(2)−Cu(1)−N(3)	79.62(10)
		N(4)−Cu(1)−O(1)	100.36(8)	Cu(1)−O(3)	2.235(2)	O(2)−Cu(1)−N(3)	104.13(10)
		N(2)−Cu(1)−N(3)	80.50(8)			O(1)−Cu(1)−N(3)	159.39(9)
						N(2)−Cu(1)−O(3)	99.11(9)
						O(2)−Cu(1)−O(3)	94.92(9)
						O(1)−Cu(1)−O(3)	90.39(8)
						N(3)−Cu(1)−O(3)	93.62(9)
^{iPrMe}L(H)$CoCl_2$ (**14**)				^{iPrMe}L(H)$ZnCl_2$ (**15**)			
Co(1)−O(1)	2.2533(17)	N(2)−Co(1)−N(3)	75.77(7)	Zn(1)−O(1)	2.2501(18)	N(2)−Zn(1)−Cl(1)	116.92(7)
Co(1)−Cl(1)	2.2579(8)	N(2)−Co(1)−Cl(2)	120.24(6)	Zn(1)−N(2)	2.074(2)	N(2)−Zn(1)−Cl(2)	124.35(7)
Co(1)−N(2)	2.0537(18)	N(3)−Co(1)−Cl(2)	105.85(5)	Zn(1)−Cl(1)	2.2304(9)	Cl(2)−Zn(1)−Cl(1)	118.26(4)
Co(1)−Cl(2)	2.2517(8)	N(2)−Co(1)−O(1)	74.15(7)	Zn(1)−Cl(2)	2.2260(8)	N(2)−Zn(1)−O(1)	74.05(7)
Co(1)−N(3)	2.2115(19)	N(3)−Co(1)−O(1)	149.65(6)	Zn(1)−N(3)	2.288(2)	Cl(2)−Zn(1)−O(1)	95.44(6)
		Cl(2)−Co(1)−O(1)	92.76(5)			Cl(1)−Zn(1)−O(1)	94.00(6)
		N(2)−Co(1)−Cl(1)	122.63(6)			N(2)−Zn(1)−N(3)	74.19(8)
		N(3)−Co(1)−Cl(1)	100.99(5)			Cl(2)−Zn(1)−N(3)	97.74(6)
		Cl(2)−Co(1)−Cl(1)	115.67(3)			Cl(1)−Zn(1)−N(3)	105.26(6)
		O(1)−Co(1)−Cl(1)	91.83(5)			O(1)−Zn(1)−N(3)	147.73(7)

[a]Estimated standard deviations are indicated in parentheses. Full lists of atomic coordinates and bond distances are available in the CIFs (Supporting Information).

X-band EPR spectra of solutions of ^{R}LCuCl (**8a**−**8c**) and ^{R}LCuOAc (**9b**,**9c**) in CH_2Cl_2/toluene (1:1 v/v) at 2−30 K exhibit rhombically distorted axial signals with resolved N-superhyperfine coupling (**8a**, **8b** in Figure 2; **8c**, **9b**, **9c**, in Figure S3, Supporting Information). Parameters from spectral simulations are listed in Table 2 (entries 1−5). These parameters compare favorably to those obtained for Cu(II) complexes of bis(arylcarboxamido)pyridine ligand **1**, as illustrated by entries 6 and 7.[1,4] From the combined data, it appears that a g_z value of ∼2.2, a large $A_{\|}$(Cu) ∼ 195 × 10^{-4} cm^{-1}, and well-resolved N-superhyperfine features are signatures of *N*,*N*′,*N*″-coordination of the supporting ligand. The only exception to this generalization is the smaller $A_{\|}$(Cu) value and lesser-resolved N-superhyperfine coupling for **8a**. With the data in hand, we can only speculate that the outlier properties of **8a** result from the reduced steric bulk of the aryl groups in this complex, perhaps enabling axial ligand interactions with the copper center (as seen in its X-ray structure) that perturb the EPR spectrum.

Cyclic voltammetry was performed on complexes ^{iPr2}LCuCl (**8b**) and ^{iPr2}LCuOAc (**9b**) to investigate the effect of the asymmetric ligand environment on the oxidation potential of neutral ^{iPr2}LCuX (X = Cl^-, OAc^-) complexes in comparison to previously studied anionic [(**1**)CuX$^-$] (R = *i*Pr, X = Cl^-)

dx.doi.org/10.1021/ic500638z | Inorg. Chem. 2014, 53, 5788−5796

Scheme 2

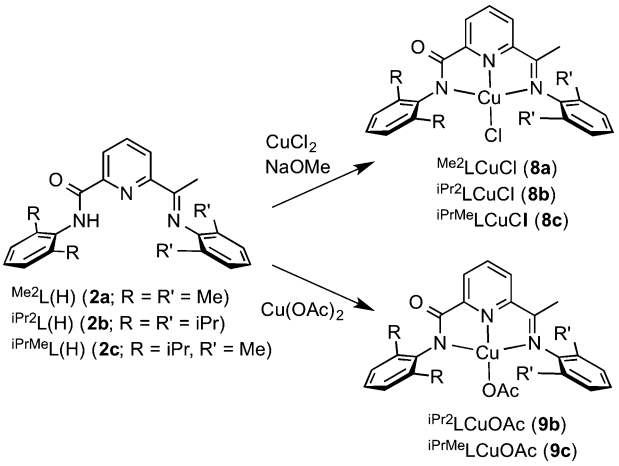

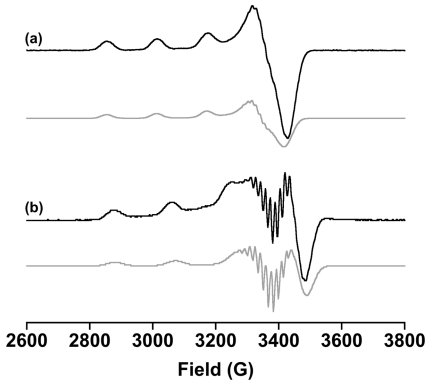

Figure 2. EPR spectra (black) and simulations (gray) of (a) ^{Me2}LCuCl (**8a**) and (b) ^{iPr2}LCuCl (**8b**). Parameters derived from the simulations are listed in Table 2.

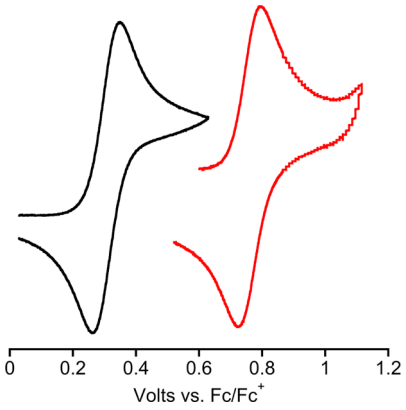

Figure 3. Cyclic voltammograms of [(**1**)CuCl]$^-$ (black trace) and ^{iPr2}LCuCl (**8b**) (red trace) all performed in acetone (0.1 M Bu_4NPF_6).

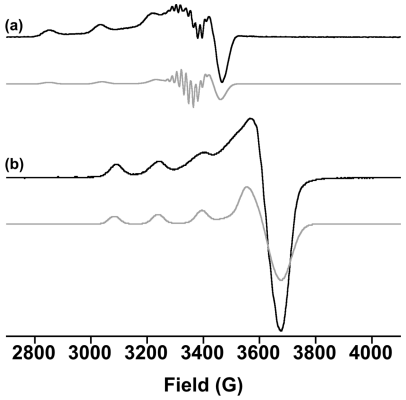

Figure 4. EPR spectra (black) and simulations (gray) of (a) ^{iPrMe}LCuOAc (**9c**) and (b) [^{iPrMe}L(H)Cu(MeCN)$_2$][$(SbF_6)_2$] (**11**). Parameters derived from the simulations are listed in Table 2.

compounds. A reversible oxidative wave was observed for ^{iPr2}LCuCl (**8b**) upon scanning anodically with $E_{1/2}$ = 0.760 V vs Fc/Fc$^+$ and ΔE_p = 62 mV (50 mV s^{-1}, 0.1 M Bu_4NPF_6 in acetone, Figure 3, red trace). In comparison to the analogous [(**1**)CuCl]$^-$ (R = *i*Pr; $E_{1/2}$ = 0.296 V vs Fc/Fc$^+$) complex, the oxidation potential of ^{iPr2}LCuCl (**8b**) is larger by almost 0.5 V (Figure 3). Data for ^{iPr2}LCuOAc (**9b**) under identical conditions (0.1 M Bu_4NPF_6 in acetone) demonstrated a slightly lower oxidation potential of $E_{1/2}$ = 0.708 V vs Fc/Fc$^+$ using scan rates of greater than 1000 mV s^{-1}; scan rates below 500 mV s^{-1} resulted in an irreversible oxidative wave (Figure S5b, Supporting Information). The observed ∼0.5 V larger oxidation potentials for ^{iPr2}LCuCl (**8b**) and ^{iPr2}LCuOAc (**9b**) relative to analogues supported by **1** support the hypothesis that installing the neutral imine donor into the ligand framework significantly raises the oxidation potential of *N,N′,N″*-copper(II) complexes.

Synthesis and Characterization of *O,N,N′*-Bound Complexes [^{R}L(H)Cu(S)$_n$][SbF_6]$_2$ (S = Solvent) and ^{iPrMe}L(H)MCl$_2$ (M = Co, Cu, Zn). In the absence of coordinating halides, a variety of solvent-labile cationic copper(II) complexes

Table 2. EPR Parameters Derived from Simulations of Experimental X-Band Spectra[a]

entry	compound	g_x	g_y	g_z	$A_{\|\|}$(Cu)	A(N$_{av}$)	A(Cl)	ref
1	^{Me2}LCuCl (**8a**)	2.08	2.05	2.23	165	12.5	12.5	[b]
2	^{iPr2}LCuCl (**8b**)	2.065	2.09	2.20	196	15	15	[b]
3	^{iPrMe}LCuCl (**8c**)	2.06	2.045	2.185	197	15	15	[b]
4	^{iPr2}LCuOAc (**9b**)	2.037	2.072	2.21	190	15		[b]
5	^{iPrMe}LCuOAc (**9c**)	2.07	2.055	2.20	194	15		[b]
6	(**1**$^{2-}$)Cu(CH$_3$CN) (R = *i*Pr)	2.027	2.064	2.190	199	15.6		1
7	(**1**$^{2-}$)Cu(MeOH) (R = Me)	2.028	2.055	2.189	193	15		4
8	[^{iPr2}L(H)Cu(MeCN)][$(SbF_6)_2$] (**10**)	2.06	2.07	2.27	165			[b]
9	[^{iPrMe}L(H)Cu(MeCN)$_2$][$(SbF_6)_2$] (**11**)	2.06	2.07	2.27	165			[b]
10	[^{iPrMe}L(H)Cu(H$_2$O)(THF)][$(SbF_6)_2$] (**12**)	2.03	2.11	2.27	155			[b]
11	^{iPrMe}L(H)CuCl$_2$ (**13**)	2.14	2.14	2.14				[b]

[a]Measured in frozen solution at 2−30 K; units of A are in 10^{-4} cm^{-1}. See the Experimental Section or indicated references for details. [b]This work.

dx.doi.org/10.1021/ic500638z | Inorg. Chem. 2014, 53, 5788−5796

with bound solvent ligands were prepared by treatment of ^{iPr2}L(H) (**2b**) or ^{iPrMe}L(H) (**2c**) with $[Cu(MeCN)_5](SbF_6)_2$ (Scheme 3). X-ray crystal structures of the complexes

Scheme 3

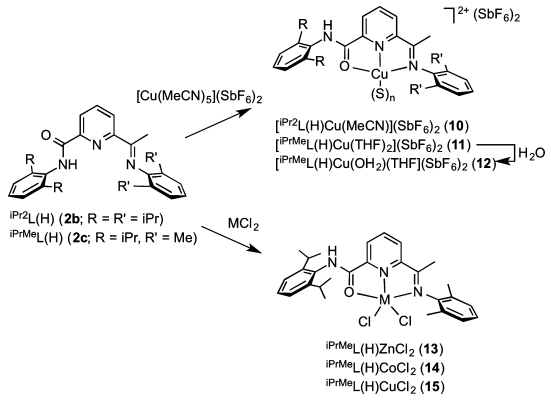

$[^{iPr2}L(H)Cu(MeCN)][(SbF_6)_2]$ (**10**, Figure 5b) and $[^{iPrMe}L(H)Cu(OH_2)(THF)][(SbF_6)_2]$ (**12**, Figure 5c) revealed tetragonal copper ion geometries with *O,N,N′*-ligation at typical Cu−O,N distances (Table 1). Metal−ligand bond distances (Table 1) are generally longer than those in the *N,N′,N″*-coordinated complexes, as expected for the differences in the protonation state of the ligands (neutral charge for *O,N,N′*- vs anionic for *N,N′,N″*-coordination). Longer axial interactions with counterions (**10**, Cu−F = 2.662(2) and 2.712(2) Å; **12**, Cu−F = 2.719(2) Å) and/or solvent molecules (**12**, Cu−O(THF) = 2.235(2) Å) are also present. Also, in **12**, two THF solvate molecules form hydrogen bonds to the bound water molecule, with H(water)−O(THF) distances of 1.788(9) and 1.802(11) Å, respectively.

Consideration of the EPR spectra for complexes **10**−**12** reveals notable differences compared to the spectra for **8** and **9**, which enable *N,N′,N″*- and *O,N,N′*-coordination to be distinguished (Table 2 and Figure S3, Supporting Information). Notably, the complexes with *O,N,N′*-coordination display larger g_z (~2.3 vs 2.2), decreased rhombicity ($g_x \sim g_y$), and smaller $A_{\parallel}$(Cu) values (160 vs ~190 × 10^{-4} cm^{-1}). In addition, N-superhyperfine coupling is not observed for any of the *O,N,N′*-copper(II) complexes. These differences are illustrated in Figure 4, in which data and simulations for ^{iPrMe}LCuOAc (**9c**) and $[^{iPrMe}L(H)Cu(MeCN)_2][(SbF_6)_2]$ (**11**) are directly compared.

Additional complexes exhibiting *O,N,N′*-coordination included $^{iPrMe}L(H)MCl_2$ (M = Cu, Co, Zn), which were generated through the combination of divalent metal ions with ^{iPrMe}L(H) (**2c**) in the absence of added base (Scheme 3). For example, treatment of ^{iPrMe}L(H) (**2c**) with MCl_2 (M = Cu, Co, Zn) yielded the neutral complexes **13**−**15**. These complexes were characterized by UV−visible spectroscopy, ESI-MS, elemental analysis, and, in the cases of **14** (M = Co) and **15** (M = Zn), by X-ray crystallography. The X-ray structures of **14** and **15** are essentially isostructural, with five-coordinate geometries illustrating *O,N,N′*-binding of the protonated forms of the arylcarboxamido(arylimino)pyridine ligand (**15** in Figure 5a; **14** in Figure S6c, Supporting Information). Coordination geometries intermediate between square-pyramidal and trigonal-bipyramidal are indicated by τ values of 0.566 (**14**) and 0.491 (**15**).[13] Consistent with the solvent-labile cationic copper(II) metal−ligand bond distances,

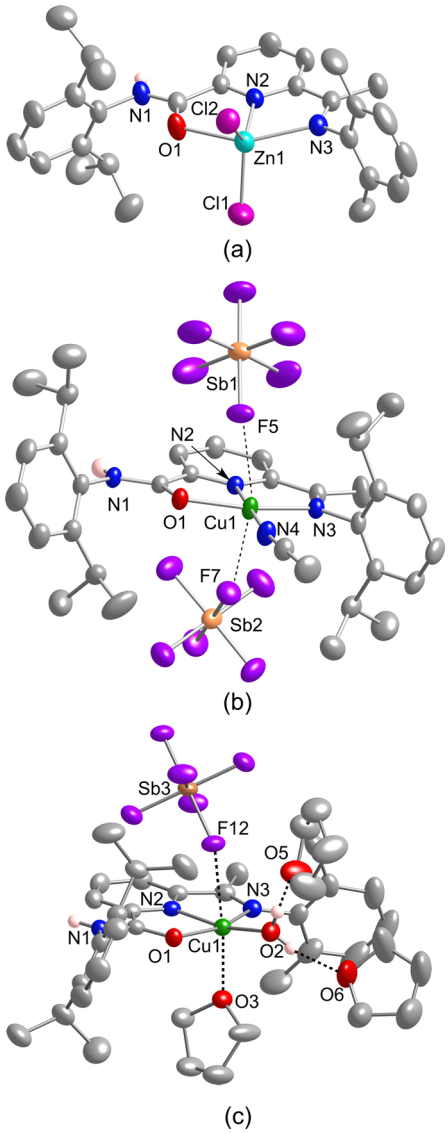

Figure 5. Representations of the X-ray crystal structures of (a) $^{iPrMe}L(H)ZnCl_2$ (**15**), (b) $[^{iPr2}L(H)Cu(MeCN)][(SbF_6)_2]$ (**10**), and (c) $[^{iPrMe}L(H)CuOH_2(THF)](SbF_6)_2$ (**12**) (omitting one SbF_6^- and showing two additional THF solvate molecules), with all non-hydrogen atoms shown as 50% thermal ellipsoids and the hydrogen atoms attached to the amide N atoms and the H_2O molecule as spheres. See Table 1 for selected interatomic distances and angles.

those in **14** and **15** are elongated relative to those in the *N,N′,N″*-coordinated complexes (Table 1). In both structures, solvent molecules in the crystal lattice propagate hydrogen-bonding networks through intermolecular interactions with the amide proton of the bound ligand ^{iPrMe}L(H) (**2c**). In the absence of suitable crystals for structure determination by X-ray diffraction, the formulation of **13** (M = Cu) is supported by CHN analysis results and the presence of a peak envelope for $[^{iPrMe}L(H)CuCl]^+$ in the ESI mass spectrum, which is consistent with the $[^{iPrMe}L(H)MCl]^+$ peaks observed for **14** and **15**.

***O,N,N′*-Carboxamide to *N,N′,N″*-Carboxamido Linkage Isomerization.** As described above, *O,N,N′*-bound complexes of L(H) or *N,N′,N″*-bound complexes of L^- may be accessed by performing the syntheses in the absence or presence of base. In addition, we have been able to demonstrate

dx.doi.org/10.1021/ic500638z | Inorg. Chem. 2014, 53, 5788−5796

that addition of base can induce conversion of the former to the latter type. Such a linkage isomerization reaction was identified by monitoring reactions of ^{iPrMe}L(H)CuCl$_2$ (**13**) with NEt$_3$ by EPR and UV−vis spectroscopy (Figures S7 and S8, Supporting Information). Preparation and analysis of a uniform series of independent frozen solution (1:1, MeCN/toluene) samples of ^{iPrMe}L(H)CuCl$_2$ (**13**) after reaction with increasing amounts of NEt$_3$ (ranging from 0 to 2 equiv of NEt$_3$) by EPR spectroscopy allowed the reaction to be monitored incrementally. Interestingly, the EPR spectra of ^{iPrMe}L(H)CuCl$_2$ (**13**) exhibit an isotropic signal, which does not vary upon preparation in various solvents and analysis under a range of temperatures (2−30 K). While this signal deviates from the previously observed spectral features for the *O,N,N′*- and *N,N′,N″*-coordinated copper(II) series of compounds, related isotropic EPR signals have been reported for similar neutral *N,N,N*-coordinated CuX$_2$ (X = Cl$^-$, ClO$_4^-$, SCN$^-$, NO$_3^-$) complexes.[14] Upon reaction of ^{iPrMe}L(H)CuCl$_2$ (**13**) with NEt$_3$, the isotropic EPR signal diminishes in intensity as features consistent with the axial signal of ^{iPrMe}LCuCl (**8c**) appear. This axial signal displays *g* and $A_{\|}$(Cu) values in agreement with the EPR spectra of independently synthesized ^{iPrMe}LCuCl (**8c**).

Consistent with this result, the progressive addition of increasing amounts of NEt$_3$ to a solution of ^{iPrMe}L(H)CuCl$_2$ (**13**) results in a color change from orange to dark green, which is characteristic of ^{iPrMe}LCuCl (**8c**). The absorption features for the latter reached maximum intensity upon addition of ∼1 equiv of NEt$_3$. Also, single crystals isolated from THF solutions of ^{iPrMe}L(H)CuCl$_2$ (**13**) after reaction with NEt$_3$ were determined to be isostructural to those obtained from independently synthesized ^{iPrMe}LCuCl (**8c**) by X-ray diffraction analysis.

CONCLUSIONS

In conclusion, we have developed a modular synthesis for the preparation of arylcarboxamido(arylimino)pyridine ligands and demonstrated their abilities to coordinate a variety of metal(II) ions (Cu, Co, and Zn). Synthetic procedures for preparation of complexes featuring anionic *N,N′,N″*-carboxamido or neutral *O,N,N′*-carboxamide ligation, as well as demonstration of linkage isomerization from *O,N,N′*- to *N,N′,N″*-coordination, have been established within these novel ligand frameworks. Extensive spectroscopic and structural characterization of a variety of metal(II) complexes in various coordination environments has provided an insight into how the asymmetric carboxamido(arylimino)pyridine framework influences the properties of these novel complexes. Ongoing investigations are focused on further establishing how these ligands support metal complexes in higher oxidation states and their potential reactivity.

EXPERIMENTAL SECTION

General. All solvents and reagents were obtained from commercial sources and used as received unless otherwise stated. The solvents tetrahydrofuran (THF), diethyl ether (Et$_2$O), toluene, pentane, and dichloromethane were passed through solvent purification columns (Glass Contour, Laguna, CA). Dichloromethane and acetonitrile were dried over CaH$_2$ and then distilled under vacuum prior to use. THF was dried over sodium/benzophenone prior to use. Acetone was dried over activated 3 Å molecular sieves and distilled under vacuum prior to use. Purified solvents were stored in a nitrogen-filled glovebox over either activated 3 Å molecular sieves or CaH$_2$ and filtered through a 0.45 μm PTFE syringe filter immediately before use. All complexes were prepared under dry nitrogen using standard Schlenk techniques or in a Vacuum Atmospheres inert atmosphere glovebox, unless otherwise stated. Cu(MeCN)$_5$(SbF$_6$)$_2$ was synthesized according to published procedures.[15] 2,6-dibromopyridine was recrystallized from benzene/*n*-heptane and dried prior to use. The synthesis of 6-acetylpyridine-2-carboxylic acid was performed according to the literature,[16] with slight modifications (see the Supporting Information for details).

Physical Methods. UV−vis spectra were recorded with an HP8453 (190−1100 nm) diode array spectrophotometer. Elemental analyses were performed by Complete Analysis Laboratories, Inc. (Parsippany, NJ) and Robertson Microlit Laboratory (Ledgewood, NJ). EPR spectra were recorded with a Bruker Continuous Wave EleXsys E500 spectrometer at either 2 or 30 K. EPR simulations were performed by using Bruker SimFonia software (version 1.25). NMR spectra were recorded on either Varian VI-300 or VXR 300 spectrometers at room temperature. Chemical shifts (δ) for ^{1}H and ^{13}C NMR spectra were referenced to residual protium in the deuterated solvent (^{1}H) or the characteristic solvent resonances of the solvent nuclei (^{13}C). ESI-MS were recorded with a Bruker BIOTOF II instrument in positive ion mode. Cyclic voltammetry was performed in a three-electrode cell with a Ag/Ag$^+$ reference electrode, a platinum auxiliary electrode, and a glassy carbon working electrode and analyzed with BASi Epsilon software. Tetrabutylammonium hexafluorophosphate (Bu$_4$NPF$_6$) was used as the supporting electrolyte. X-ray crystallography data collections and structure solutions were conducted by using either Siemens SMART or Bruker APEX II CCD instruments and the current SHELXTL suite of programs.[17]

6-Acetyl-*N*-(2,6-diisopropylphenyl)picolinamide (7a). 6-Acetyl-2-pyridinecarboxylic acid (1.69 g, 10.3 mmol) was dissolved in toluene (100 mL), treated with oxalyl chloride (1.39 mL, 16.5 mmol), and refluxed 16 h under N$_2$. The solvent was removed *in vacuo* after cooling the mixture to room temperature. The resulting brown solid and 2,6-diisopropyl aniline hydrochloride salt (1.1 equiv, 2.4 g, 11.3 mmol) were dissolved in THF (75 mL) and cooled to 0 °C under N$_2$. Triethylamine (2.5 equiv, 3.6 mL, 25.7 mmol) was then added via syringe, resulting in the immediate formation of a white precipitate. After stirring for 15 min at 0 °C, the reaction mixture was warmed to room temperature and subsequently brought to reflux for 2 h. After cooling to room temperature, the reaction mixture was filtered and the resulting brown filtrate was concentrated by rotary evaporation. The resulting residue was then washed with hexanes to yield a brown solid and isolated via filtration. The brown solid was then dissolved in a 10:90% EtOAc:pentane solution and passed through charcoal. Evaporation of the resulting filtrate yielded a white solid (2.46 g, 74%). ^{1}H NMR (300 MHz, CD$_2$Cl$_2$): δ_H 9.35 (br s, 1H, N*H*), 8.43 (d, 1H, *J* = 8.4 Hz, Py H), 8.23 (d, 1H, *J* = 7.5 Hz, Py H), 8.10 (t, 1H, *J* = 7.8 Hz, Py H), 7.37 (t, 1H, *J* = 7.6 Hz, Ar H), 7.26 (d, 2H, *J* = 7.2 Hz, Ar H), 3.14 (m, 2H, Ar C*H*(CH$_3$)$_2$), 2.77 (s, 3H, C(O)C*H*$_3$), 1.22 (d, 12 H, *J* = 6.9 Hz, Ar CH(C*H*$_3$)$_2$). ^{13}C NMR (300 MHz, CD$_2$Cl$_2$): δ_C 23.9, 26.1, 29.5, 124.1, 124.6, 126.3, 128.9, 131.9, 139.5, 146.9, 149.7, 152.6, 163.4, 199.0. Anal. Calcd for C$_{20}$H$_{24}$N$_2$O$_2$: C 74.04, H 7.46, N 8.64. Found: C 73.96, H 7.29, N 8.55.

6-Acetyl-*N*-(2,6-dimethylphenyl)picolinamide (7b). **7b** was synthesized following the identical procedure as was used for **7a**, except with the substitution of 2,6-dimethylaniline for 2,6-diisopropyl aniline (1.92 g, 70%). ^{1}H NMR (300 MHz, CD$_2$Cl$_2$): δ_H 9.43 (br s, 1H, N*H*); 8.44 (d, 1H, *J* = 7.5 Hz, Py H), 8.22 (d, 1H, *J* = 7.8 Hz, Py H), 8.10 (t, 1H, *J* = 7.8 Hz, Py H), 7.17 (br s, 3H, Ar H), 2.78 (s, 3H, C(O)C*H*$_3$), 2.31 (s, 6H, Ar CH(C*H*$_3$)$_2$). ^{13}C NMR (300 MHz, CD$_2$Cl$_2$): δ_C 18.8, 26.1, 124.5, 126.2, 127.8, 128.7, 134.5, 136.0, 139.4, 149.8, 152.6, 162.1, 199.0. Anal. Calcd for C$_{16}$H$_{16}$N$_2$O$_2$: C 71.62, H 6.01, N 10.44. Found: C 71.71, H 6.01, N 10.40.

^{Me2}L(H) (2a). **2a** was synthesized following the identical procedure as was used for **2b**, except starting from **7b** instead of **7a** (1.43 g, 48%). ^{1}H NMR (300 MHz, CD$_2$Cl$_2$): δ_H 9.50 (br s, 1H, N*H*), 8.62 (d, 1H, *J* = 7.8 Hz, Py H), 8.35 (d, 1H, *J* = 6.6 Hz, Py H), 8.07 (t, 1H, *J* = 7.8 Hz, Py H), 7.16−6.92 (m, 6H, Ar H), 2.31 (s, 6H, Ar CH(C*H*$_3$)$_2$, *N*-arylcarboxamide), 2.23 (s, 3H, N=CC*H*$_3$), 2.04 (s, 6H, Ar CH(C*H*$_3$)$_2$, *N*-arylimine). ^{13}C NMR (300 MHz, CD$_2$Cl$_2$): δ_C 16.8, 18.2, 18.9, 123.7, 124.0, 124.4, 125.8, 127.7, 128.4, 128.6, 136.0, 138.7,

dx.doi.org/10.1021/ic500638z | Inorg. Chem. 2014, 53, 5788−5796

155.5, 176.7. Anal. Calcd for $C_{24}H_{25}N_3O$: C 77.60, H 6.78, N 11.31. Found: C 77.49, H 6.69, N 11.40

^{iPr2}L(H) (2b). A solution of 2,6-diisopropylaniline (3.7 mL, 19.8 mmol) was dissolved in 100 mL of toluene and cooled to 0 °C under N_2. $TiCl_4$ (0.36 mL, 3.3 mmol) was added via syringe, and the resulting cloudy brown solution was stirred for 2 h. After warming the solution to room temperature, a solution of **7a** (2.14 g, 6.6 mmol) in 40 mL of toluene was added to the reaction. The reaction mixture was then refluxed for 16 h. After cooling to room temperature, Et_2O (100 mL) was added and the reaction mixture was stirred for 15 min. The reaction mixture was then filtered through Celite, and the brown-yellow filtrate was concentrated via rotary evaporation. The resulting brown-yellow solid was purified by column chromatography on silica gel (EtOAc/pentane (1:10); R_f = 0.36) to yield a yellow solid (2.02 g, 63%). The ^{1}H NMR and high-resolution ESI-MS of **2b** are previously reported[3] and correlate well with the current data. ^{1}H NMR (300 MHz, CD_2Cl_2): δ_H 9.45 (br s, 1H, N*H*), 8.61 (d, 1H, *J* = 7.8 Hz, Py H), 8.36 (d, 1H, *J* = 7.5 Hz, Py H), 8.08 (t, 1H, *J* = 7.8 Hz, Py H), 7.39−7.08 (m, 6H, Ar H), 3.17 (m, 2H, Ar C*H*$(CH_3)_2$, *N*-arylcarboxamide), 2.76 (m, 2H, Ar C*H*$(CH_3)_2$, *N*-arylimine), 2.26 (s, 3H, N=CCH_3), 1.24−1.14 (m, 24 H, Ar CH(CH_3)$_2$). ^{13}C NMR (300 MHz, CD_2Cl_2): δ_C 17.5, 23.1, 23.5, 23.9, 28.9, 29.5, 30.3, 123.6, 124.1, 124.1, 124.4, 124.5, 128.8, 132.1, 136.2, 138.8, 146.7, 146.9, 149.3, 155.5, 163.9, 166.4. Anal. Calcd for $C_{32}H_{41}N_3O$: C 79.46, H 8.54, N 8.69. Found: C 79.42, H 8.66, N 8.51.

^{iPrMe}L(H) (2c). **2c** was synthesized following the identical procedure as was used for **2b**, except using 2,6-dimethylaniline instead of 2,6-diisopropylaniline (1.81 g, 64%). Single crystals suitable for X-ray diffraction were obtained from slow evaporation of a concentrated CH_2Cl_2 solution at room temperature. ^{1}H NMR (300 MHz, CD_2Cl_2): δ_H 9.45 (br s, 1H, N*H*), 8.63 (d, 1H, *J* = 7.8 Hz, Py H), 8.36 (d, 1H, *J* = 7.5, Py H), 8.08 (t, 1H, *J* = 7.8 Hz, Py H), 7.39−6.93 (m, 6H, Ar *H*), 3.17 (m, 2H, Ar C*H*$(CH_3)_2$), 2.23 (s, 3H, N=CCH_3), 2.05 (s, 6H, Ar CH(CH_3)$_2$, *N*-arylimine), 1.24 (d, 12H, *J* = 6.9 Hz, Ar CH(CH_3)$_2$, *N*-arylcarboxamide).^{13}C NMR (300 MHz, CD_2Cl_2): δ_C 16.8, 18.2, 23.9, 29.5, 123.7, 124.1, 124.1, 124.5, 125.8, 128.4, 128.8, 132.1, 138.7, 146.9, 149.1, 149.3, 155.5, 163.9, 166.5. Anal. Calcd for $C_{28}H_{33}N_3O$: C 78.65, H 7.78, N 9.83. Found: C 78.59, H 7.80, N 9.79.

^{Me2}LCuCl (8a). **8a** was synthesized analogously to **8b** and **8c**, except using **2a** instead of **2b** and the reaction time was shortened to 30 min (longer times resulted in lower yields) (0.111 g, 76%). Single crystals suitable for X-ray diffraction were obtained from diffusion of Et_2O into a concentrated MeCN solution at −20 °C. MS (ESI+, CH_3OH): *m*/*z* = 490.64 [**8a** + Na^+]$^+$. UV−vis (CH_2Cl_2) λ_{max} (ε, M^{-1} cm^{-1}): 435 (1964); 655 (348) nm. EPR [9.64 GHz, THF/toluene (1:1), 2 K]: g_x = 2.08, g_y = 2.05, g_z = 2.23; $A_\parallel$(Cu): 165 × 10^{-4} cm^{-1}; *A*(N): 12.5 × 10^{-4} cm^{-1}; *A*(Cl): 12.5 × 10^{-4} cm^{-1}. Unfortunately, repeated attempts to obtain satisfactory CHN analysis were unsuccessful.

^{iPr2}LCuCl (8b). Anhydrous $CuCl_2$ (0.0353 g, 0.263 mmol) and **2b** (0.1156 g, 0.239 mmol) were placed in a 100 mL round-bottom flask and dissolved in 20 mL of THF, forming a golden brown solution. Sodium methoxide (0.5 M in MeOH, 0.57 mL, 0.287 mmol) was added, causing the solution to turn dark green with a light-colored precipitate. After stirring for 16 h, the reaction was filtered and the solvent was removed via rotary evaporation. The resulting green residue was dissolved in CH_2Cl_2 (10 mL) and filtered to remove any insoluble material. Pentane (50 mL) was then added, and the mixture was placed in a −20 °C freezer for several hours. The resulting green solid was isolated by vacuum filtration (0.101 g, 73%). Single crystals suitable for X-ray diffraction were obtained from diffusion of pentane into a concentrated CH_2Cl_2 solution at −20 °C. MS (ESI+, CH_3OH): *m*/*z* = 581.16 [**8b** + Na^+]$^+$. UV−vis (CH_2Cl_2) λ_{max} (ε, M^{-1} cm^{-1}): 440 (1785); 675 (260) nm. EPR [9.64 GHz, CH_2Cl_2/toluene (1:1), 2 K]: g_x = 2.065, g_y = 2.090, g_z = 2.200; $A_\parallel$(Cu): 196 × 10^{-4} cm^{-1}; *A*(N): 15 × 10^{-4} cm^{-1}; *A*(Cl): 15 × 10^{-4} cm^{-1}. Anal. Calcd for $C_{32}H_{40}ClCuN_3O$: C 66.07, H 6.93, N 7.22. Found: C 65.98, H 6.89, N 7.13.

^{iPrMe}LCuCl (8c). **8c** was synthesized following an identical procedure as was used for **8b**, except using **2c** instead of **2b** (0.0989 g, 70%). Single crystals suitable for X-ray diffraction were obtained from diffusion of pentane into a concentrated CH_2Cl_2 solution at −20 °C. MS (ESI+, CH_3OH): *m*/*z* = 548.24 [**8c** + Na^+]$^+$. UV−vis (CH_2Cl_2) λ_{max} (ε, M^{-1} cm^{-1}): 435 (1976); 660 (346) nm. EPR [9.64 GHz, CH_2Cl_2/toluene (1:1), 2 K]: g_x = 2.060, g_y = 2.045, g_z = 2.185; $A_\parallel$(Cu): 197 × 10^{-4} cm^{-1}; *A*(N): 15 × 10^{-4} cm^{-1}, *A*(Cl): 15 × 10^{-4} cm^{-1}. Anal. Calcd for $C_{28}H_{32}ClCuN_3O$: C 63.99, H 6.14, N 8.00. Found: C 63.85, H 6.04, N 7.94.

^{iPr2}LCuOAc (9b). A suspension of **2b** (100 mg, 0.21 mmol) and $Cu(OAc)_2{\cdot}H_2O$ (45 mg, 0.23 mmol) in 50 mL of MeCN was heated to reflux for 2 h, resulting in a dark green solution. Upon cooling to room temperature, the reaction was stirred with $MgSO_4$ for 30 min. The reaction mixture was then filtered, and the solvent was removed via rotary evaporation to yield a dark green solid (0.0964 g, 77%). Single crystals suitable for X-ray diffraction were obtained from diffusion of pentane into a concentrated CH_2Cl_2 solution at −20 °C. MS (ESI+, CH_3OH): *m*/*z* = 545.21 [**9b** − OAc^-]$^+$. UV−vis (CH_2Cl_2) λ_{max} (ε, M^{-1} cm^{-1}): 385 (1972); 655 (275) nm. EPR [9.64 GHz, DCM/toluene (1:1), 30 K]: g_x = 2.0375, g_y = 2.0725, g_z = 2.2100; $A_\parallel$(Cu): 190 × 10^{-4} cm^{-1}, *A*(N): 15 × 10^{-4} cm^{-1}. Anal. Calcd for $C_{34}H_{43}CuN_3O_3$: C 67.47, H 7.16, N 6.94. Found: C 67.43, H 7.17, N 6.85.

^{iPrMe}LCuOAc (9c). **9c** was synthesized as for **9b**, except using **2c** instead of **2b**. Single crystals suitable for X-ray diffraction were obtained from diffusion of pentane into a concentrated CH_2Cl_2 solution at −20 °C (0.103 g, 80%). MS (ESI+, CH_3OH): *m*/*z* = 489.13 [**9c** − OAc^-]$^+$. UV−vis (acetone) λ_{max} (ε, M^{-1} cm^{-1}): 375 (1860); 645 (343) nm. EPR [9.64 GHz, CH_2Cl_2/toluene (1:1), 2 K]: g_x = 2.070, g_y = 2.055, g_z = 2.200; $A_\parallel$(Cu): 194 × 10^{-4} cm^{-1}, *A*(N): 15 × 10^{-4} cm^{-1}. Anal. Calcd for $C_{30}H_{35}CuN_3O_3$: C 65.61, H 6.42, N 7.65. Found: C 65.49, H 6.41, N 7.54.

[^{iPr2}L(H)Cu(MeCN)][$(SbF_6)_2$] (10). $Cu(MeCN)_5(SbF_6)_2$ (81 mg, 0.10 mmol) and **2b** (50 mg, 0.11 mmol) were combined in 4 mL of THF. After stirring for 30 min, pentane (10 mL) was added. A green solid precipitated and was isolated by vacuum filtration. The resulting green powder was washed with pentane (3 × 10 mL) and dried under vacuum for 1 h (0.767 g, 70%). Single crystals suitable for X-ray diffraction were obtained from diffusion of pentane into a concentrated CH_2Cl_2 solution at −30 °C. MS (ESI+, CH_3OH): *m*/*z* = 545.23 [^{iPr2}LCu$^+$]$^+$. UV−vis (CH_2Cl_2) λ_{max} (ε, M^{-1} cm^{-1}): 428 (1864); 665 (463) nm. EPR [9.64 GHz, CH_2Cl_2/toluene (1:1), 30 K]: g_x = 2.06, g_y = 2.07, g_z = 2.27; $A_\parallel$(Cu): 165 × 10^{-4} cm^{-1}. Anal. Calcd for $C_{32}H_{41}N_3OCuSb_2F_{12}$ (^{iPr2}L(H)Cu; the MeCN ligand was lost upon drying of the crystals under vacuum prior to analysis): C 37.73, H 4.06, N 4.12. Found: C 37.43, H 4.26, N 4.76.

[^{iPrMe}L(H)Cu(MeCN)$_2$][$(SbF_6)_2$] (11). **11** was synthesized following the procedure as was used for **10** except **2c** was used in place of **2b** (0.0890 g, 73%). MS (ESI+, CH_3OH): *m*/*z* = 489.18 [^{iPrMe}LCu$^+$]$^+$. UV−vis (CH_2Cl_2) λ_{max} (ε, M^{-1} cm^{-1}): 415 (1060); 690 (215) nm. EPR [9.64 GHz, CH_2Cl_2/toluene (1:1), 30 K]: g_x = 2.06, g_y = 2.07, g_z = 2.27; $A_\parallel$(Cu): 165 × 10^{-4} cm^{-1}. Anal. Calcd for $C_{32}H_{39}N_5OCuSb_2F_{12}$: C 36.79, H 3.76, N 6.70. Found: C 36.73, H 3.81, N 6.44.

[^{iPrMe}L(H)Cu(H_2O)THF][$(SbF_6)_2$] (12). $Cu(MeCN)_5(SbF_6)_2$ (93 mg, 0.12 mmol) and **2c** (57 mg, 0.12 mmol) were combined in 4 mL of THF in a glovebox. After stirring for 30 min, the reaction was removed from the glovebox and 10 mL of wet solvent (THF) was added to the reaction mixture. The reaction was allowed to continue stirring for 1 h, after which the solvent was removed. The resulting green residue was taken up in 5 mL of THF, and pentane (100 mL) was added to the flask. A green solid resulted after several hours of storage at −20 °C. The solid was isolated via vacuum filtration and washed with pentane (3 × 10 mL). Single crystals suitable for X-ray diffraction were obtained from diffusion of pentane into a concentrated CH_2Cl_2 solution at −20 °C (0.0884 g, 63%). MS (ESI+, CH_3OH): *m*/*z* = 489.21 [^{iPrMe}LCu$^+$]$^+$. UV−vis (CH_2Cl_2) λ_{max} (ε, M^{-1} cm^{-1}): 410 (2395); 695 (375) nm. ESI-MS: *m*/*z* 489.22 [^{i}PrMeLCu$^+$]$^+$. EPR [9.64 GHz, THF/toluene (1:1), 30 K]: g_x = 2.03, g_y = 2.11, g_z = 2.27; $A_\parallel$(Cu): 155 × 10^{-4} cm^{-1}. Anal. Calcd for $C_{32}H_{43}CuF_{12}N_3O_3Sb_2$: C 36.51, H 4.12, N 3.99. Found: C 36.60, H 4.29, N 3.76.

^{iPrMe}L(H)$CuCl_2$ (13). Anhydrous $CuCl_2$ (16 mg, 0.12 mmol) and **2c** (50 mg, 0.12 mmol) were combined in 4 mL of MeCN. The solution

dx.doi.org/10.1021/ic500638z | Inorg. Chem. 2014, 53, 5788−5796

was stirred at room temperature for 30 min, resulting in an orange-brown solution. Et_2O (12 mL) was added to the solution, which was then cooled to −30 °C. The resulting orange-brown solid was collected by vacuum filtration, washed with pentane (3 × 10 mL), and dried under vacuum for 1 h (0.0624 g, 95%). MS (ESI+, CH_3OH): m/z = 525.27 [**13** − Cl^-]$^+$. UV−vis (MeCN) λ_{max} (ε, M^{-1} cm^{-1}): 400(sh) (726); 450 (700); 890 (94) nm. EPR [9.64 GHz, MeCN/toluene (1:1), 30 K]: $g_{x,y,z}$ = 2.14. Anal. Calcd for $C_{28}H_{33}Cl_2N_3OCu$: C 59.84, H 5.92, N 7.48. Found: C 59.71, H 5.82, N 7.46.

^{iPrMe}L(H)CoCl$_2$ (14). $CoCl_2$ (16 mg, 0.12 mmol) and **2c** (53 mg, 0.12 mmol) were stirred in 10 mL of a 1:1 acetone/MeCN mixture to yield a bright green solution. After stirring for 2 h, the reaction mixture was filtered and the filtrate was concentrated to approximately 2 mL total volume. Et_2O (10 mL) was added to the solution, which was then cooled to −30 °C. The resulting green powder was collected by vacuum filtration, washed with pentane (3 × 10 mL), and dried under vacuum for 1 h (0.0463 g, 71%). Single crystals suitable for X-ray diffraction were obtained from diffusion of Et_2O into a concentrated MeCN solution at −30 °C. MS (ESI+, CH_3CN): m/z = 521.06 [**14** − Cl^-]$^+$. UV−vis (MeCN) λ_{max} (ε, M^{-1} cm^{-1}): 590 (230); 685 (303) nm. Anal. Calcd for $C_{28}H_{33}Cl_2N_3OCo$: C 60.33, H 5.97, N 7.54. Found: C 60.18, H 5.87, N 7.45.

^{iPrMe}L(H)ZnCl$_2$ (15). $ZnCl_2$ (16 mg, 0.12 mmol) and **2c** (50 mg, 0.12 mmol) were dissolved in 4 mL of THF. After stirring for 15 min, a light colored precipitate formed in the solution. The solid was collected by vacuum filtration, washed with pentane (3 × 10 mL), and dried under vacuum for 1 h (0.0488 g, 74%). Single crystals suitable for X-ray diffraction were obtained from diffusion of Et_2O into a concentrated MeCN solution at −30 °C. ^{1}H NMR (300 MHz, $(CD_3)_2SO$): δ_H 10.18 (br s, 1H, N*H*); 8.55 (d, 1H, J = 7.5 Hz, Py H), 8.24−8.18 (m, 2H, Py H), 7.36−6.90 (m, 6H, Ar H), 3.11 (m, 2H, Ar C*H*$(CH_3)_2$), 2.94 (s, 3H, N=CC*H*$_3$), 1.99 (s, 6H, Ar CH(C*H*$_3$)$_2$, *N*-arylimine), 1.15 (d, 12H, J = 6.6 Hz, Ar CH(C*H*$_3$)$_2$, *N*-arylcarboxamide). MS (ESI+, CH_3CN): m/z = 526.17 [**15** − Cl^-]$^+$. Anal. Calcd for $C_{28}H_{33}Cl_2N_3OZn$: C 59.64, H 5.90, N 7.45. Found: C 59.58, H 5.78, N 7.35.

■ ASSOCIATED CONTENT

Ⓢ Supporting Information

Selected spectroscopic and ESI-MS data (PDF) and X-ray data (CIF). This material is available free of charge via the Internet at http://pubs.acs.org.

■ AUTHOR INFORMATION

Corresponding Author

*E-mail: wtolman@umn.edu.

Notes

The authors declare no competing financial interest.

■ ACKNOWLEDGMENTS

We thank the National Institutes of Health for financial support of this research (R37GM47365 to W.B. T.). The authors thank Benjamin D. Neisen and Gereon M. Yee for assistance in collecting EPR spectra, Dr. Patrick J. Donoghue for synthesis and cyclic voltammetry characterization of [NBu_4][(**1**)CuCl], and Dr. Victor G. Young, Jr., for assistance with X-ray crystallography. Some experiments reported in this paper were performed at the Biophysical Spectroscopy Center in the University of Minnesota Department of Biochemistry, Molecular Biology, and Biophysics.

■ REFERENCES

(1) Donoghue, P. J.; Gupta, A. K.; Boyce, D. W.; Cramer, C. J.; Tolman, W. B. *J. Am. Chem. Soc.* **2010**, *132*, 15869−15871.

(2) Pirovano, P.; Magherusan, A. M.; McGlynn, C.; Ure, A.; Lynes, A.; McDonald, A. R. *Angew. Chem., Int. Ed.* **2014**, DOI: 10.1002/anie.201311152.

(3) (a) Huang, D.; Holm, R. H. *J. Am. Chem. Soc.* **2010**, *132*, 4693−4701. (b) Huang, D.; Makhlynets, O. V.; Tan, L. L.; Lee, S. C.; Rybak-Akimova, E. V.; Holm, R. H. *Inorg. Chem.* **2011**, *50*, 10070−10081. (c) Huang, D.; Makhlynets, O. V.; Tan, L. L.; Lee, S. C.; Rybak-Akimova, E. V.; Holm, R. H. *Proc. Natl. Acad. Sci. U.S.A.* **2011**, *108*, 1222−1227. (d) Zhang, X.; Huang, D.; Chen, Y.-S.; Holm, R. H. *Inorg. Chem.* **2012**, *51*, 11017−11029.

(4) Tehranchi, J.; Donoghue, P. J.; Cramer, C. J.; Tolman, W. B. *Eur. J. Inorg. Chem.* **2013**, 4077−4084.

(5) Donoghue, P. J.; Tehranchi, J.; Cramer, C. J.; Sarangi, R.; Solomon, E. I.; Tolman, W. B. *J. Am. Chem. Soc.* **2011**, *133*, 17602−17605.

(6) Selected recent examples: (a) Bowman, A. C.; Milsmann, C.; Bill, E.; Turner, Z. R.; Lobkovsky, E.; DeBeer, S.; Wieghardt, K.; Chirik, P. J. *J. Am. Chem. Soc.* **2011**, *133*, 17353−17369. (b) Darmon, J. M.; Stieber, S. C. E.; Sylvester, K. T.; Fernández, I.; Lobkovsky, E.; Semproni, S. P.; Bill, E.; Wieghardt, K.; DeBeer, S.; Chirik, P. J. *J. Am. Chem. Soc.* **2012**, *134*, 17125−17137. (c) Darmon, J. M.; Turner, Z. R.; Lobkovsky, E.; Chirik, P. J. *Organometallics* **2012**, *31*, 2275−2285. (d) Hojilla Atienza, C. C.; Tondreau, A. M.; Weller, K. J.; Lewis, K. M.; Cruse, R. W.; Nye, S. A.; Boyer, J. L.; Delis, J. G. P.; Chirik, P. J. *ACS Catal.* **2012**, *2*, 2169−2172. (e) Stieber, S. C. E.; Milsmann, C.; Hoyt, J. M.; Turner, Z. R.; Finkelstein, K. D.; Wieghardt, K.; DeBeer, S.; Chirik, P. J. *Inorg. Chem.* **2012**, *51*, 3770−3785. (f) Tondreau, A. M.; Atienza, C. C. H.; Darmon, J. M.; Milsmann, C.; Hoyt, H. M.; Weller, K. J.; Nye, S. A.; Lewis, K. M.; Boyer, J.; Delis, J. G. P.; Lobkovsky, E.; Chirik, P. J. *Organometallics* **2012**, *31*, 4886−4893. (g) Tondreau, A. M.; Stieber, S. C. E.; Milsmann, C.; Lobkovsky, E.; Weyhermüller, T.; Semproni, S. P.; Chirik, P. J. *Inorg. Chem.* **2012**, *52*, 635−646. (h) Yu, R. P.; Darmon, J. M.; Hoyt, J. M.; Margulieux, G. W.; Turner, Z. R.; Chirik, P. J. *ACS Catal.* **2012**, *2*, 1760−1764. (i) Hojilla Atienza, C. C.; Milsmann, C.; Semproni, S. P.; Turner, Z. R.; Chirik, P. J. *Inorg. Chem.* **2013**, *52*, 5403−5417. (j) Hoyt, J. M.; Sylvester, K. T.; Semproni, S. P.; Chirik, P. J. *J. Am. Chem. Soc.* **2013**, *135*, 4862−4877.

(7) (a) Fan, R.-Q.; Wang, P.; Yang, Y.-L.; Zhang, Y.-J.; Yin, Y.-B.; Hasi, W. *Polyhedron* **2010**, *29*, 2862−2866. (b) Le Gall, B.; Conan, F.; Cosquer, N.; Kerbaol, J.-M.; Sala-Pala, J.; Kubicki, M. M.; Vigier, E.; Gomez-Garcia, C. J.; Molinié, P. *Inorg. Chim. Acta* **2005**, *358*, 2513−2522. (c) Le Gall, B.; Conan, F.; Cosquer, N.; Kerbaol, J.-M.; Kubicki, M. M.; Vigier, E.; Le Mest, Y.; Sala-Pala, J. *Inorg. Chim. Acta* **2001**, *324*, 300−308.

(8) Manuel, T. D.; Rohde, J.-U. *J. Am. Chem. Soc.* **2009**, *131*, 15582−15583.

(9) (a) Zhang, W.; Wang, Y.; Yu, J.; Redshaw, C.; Hao, X.; Sun, W.-H. *Dalton Trans.* **2011**, *40*, 12856−12865. (b) Shen, M.; Sun, W.-H. *Appl. Organomet. Chem.* **2009**, *23*, 51−54. (c) Shen, M.; Hao, P.; Sun, W.-H. *J. Organomet. Chem.* **2008**, *693*, 1683−1695.

(10) Cabell, L. A.; Best, M. D.; Lavigne, J. J.; Schneider, S. E.; Perreault, D. M.; Monahan, M.-K.; Anslyn, E. V. *J. Chem. Soc., Perkin Trans. 2* **2001**, 315−323.

(11) Scott, J.; Vidyaratne, I.; Korobkov, I.; Gambarotta, S.; Budzelaar, P. H. M. *Inorg. Chem.* **2008**, *47*, 896−911.

(12) Wang, D.; Lindeman, S. V.; Fiedler, A. T. *Eur. J. Inorg. Chem.* **2013**, 4473−4484 and references therein.

(13) Addison, A. W.; Rao, T. N.; Reedjik, J.; van Rijn, J.; Verschoor, G. C. *J. Chem. Soc., Dalton Trans.* **1984**, 1349−1356.

(14) Selected examples: (a) Foster, C. L.; Kilner, C. A.; Thornton-Pett, M.; Halcrow, M. A. *Polyhedron* **2002**, *21*, 1031−1041. (b) Balamurugan, R.; Palaniandavar, M.; Halcrow, M. A. *Polyhedron* **2006**, *25*, 1077−1088. (c) Sharma, A. K.; Mukherjee, R. *Inorg. Chim. Acta* **2008**, *361*, 2768−2776. (d) Manikandan, P.; Thomas, K. R. J.; Manoharan, P. T. *J. Chem. Soc., Dalton Trans.* **2000**, *24*, 2779−2785.

(15) (a) Leboeuf, D.; Huang, J.; Gandon, V.; Frontier, A. J. *Angew. Chem., Int. Ed.* **2011**, *50*, 10981−10985. (b) Baxter, A. C.; Cameron, J.

H.; McAuley, A.; McLaren, F. M.; Winfield, J. M. *J. Fluor. Chem.* **1977**, *10*, 289−298.
(16) Ronson, T. K.; Adams, H.; Harding, L. P.; Pope, S. J. A.; Sykes, D.; Faulkner, S.; Ward, M. D. *Dalton Trans.* **2007**, *47*, 1006−1022.
(17) *SHELXTL*, v. 6.14; Bruker Analytical X-ray Systems: Madison, WI, 2000.